Calculated Neutron and Gamma Irradiation Response of Actively Cooled Mirrors for Laser Fusion Power Reactors

M.M.H. Ragheb and C.W. Maynard

October 1977

UWFDM-218

FUSION TECHNOLOGY INSTITUTE

UNIVERSITY OF WISCONSIN

MADISON WISCONSIN

Calculated Neutron and Gamma Irradiation Response of Actively Cooled Mirrors for Laser Fusion Power Reactors

M.M.H. Ragheb and C.W. Maynard

Fusion Technology Institute
University of Wisconsin
1500 Engineering Drive
Madison, WI 53706

http://fti.neep.wisc.edu

October 1977

UWFDM-218

"LEGAL NOTICE"

"This work was prepared by the University of Wisconsin as an account of work sponsored by the Electric Power Research Institute, Inc. ("EPRI"). Neither EPRI, members of EPRI, the University of Wisconsin, nor any person acting on behalf of either:

"a. Makes any warranty or representation, express or implied, with respect to the accuracy, completeness, or usefulness of the information contained in this report, or that the use of any information, apparatus, method, or process disclosed in this report may not infringe privately owned rights; or

"b. Assumes any liabilities with respect to the use of, or for damages resulting from the use of, any information, apparatus, method or process disclosed in this report."

CALCULATED NEUTRON AND GAMMA IRRADIATION RESPONSE OF ACTIVELY COOLED MIRRORS FOR LASER FUSION POWER REACTORS

Magdi M. H. Ragheb

Charles W. Maynard

November 1977

UWFDM-218

Fusion Technology Program
Nuclear Engineering Department
University of Wisconsin
Madison, Wisconsin 53706, USA

TABLE OF CONTENTS

CALCULATED NEUTRON AND GAMMA IRRADIATION RESPONSE OF ACTIVELY COOLED MIRRORS FOR LASER FUSION POWER REACTORS

ABSTRACT

The calculated neutron and gamma irradiation response of water cooled mirrors for Laser Fusion Power Reactors, for some candidate structural materials is compared. Such a response affects the mirror bulk structure, whereas pellet X-rays and debris affect just the first few microns of its surface. The highest atomic displacements (dpa) occur in Cu, hydrogen gas production in Fe, and helium gas production in Al. The lowest values for all these occur in Mo. The highest volumetric neutron and gamma heating rates occur in Cu, the lowest in Al. Variations of the obtained estimates are within one order of magnitude for different materials. At the back-side of the mirror, materials responses agree in relative magnitude with previous results for first wall materials and blanket spectra, but differ at the mirror face where the response to the 14-Mev neutron component predominates.

ACKNOWLEDGEMENT

Thanks are due to Mr. H. Avci, Dr. E. Cheng, and Mr. T. Wu for making some cross-sections data available for the calculations, to Professor W. Wolfer and to Mr. T. Hunter for some helpful discussions. The excellent typing of Ms. Veronica Smart is gratefully acknowledged. This work was partially supported by the Electric Power Research Institute (EPRI).

FIGURE CAPTIONS

LIST OF TABLES

1. INTRODUCTION

This work presents a comparison of the calculated neutron and gamma irradiation response of candidate materials for water cooled mirrors for Laser Fusion Power Reactors. Active cooling of the last optical element is a necessity in a reactor environment even though not considered in current experiments, to avoid the excessive heating and the distortion which may be caused by the thermal gradients generated by neutron and gamma heating, laser light, and pellet alpha and X-ray radiation. A honeycomb structure cooled with water will also act as an effective shield for the concrete behind the mirrors to the 14-Mev neutrons directly reaching the mirror and the generated secondary gamma rays, and provide inertia to damp plant vibrations. Whereas pellet X-rays and debris will affect just the first few microns at the mirror surface, neutron and secondary gammas will affect the bulk of the mirror structure.

Mirror blanks can be fabricated from brazed or welded box structures. Mirror faces can be clad with copper either by electroplating or by brazing a thin copper sheet to the substrate [1]. Reichelt et al. [15] discussed mirror materials constraints and choices, as well as fabrication techniques, and recommended the use of electroplated copper on aluminum. For the structural materials, cost eliminates materials such as beryllium, that are desirable as to their thermal distortion, rigidity, and stiffness-to-weight ratio. Beryllium is also undesirable as a mirror material, because of its (n,2n) reaction with the 14-Mev neutrons. Molybdenum has an acceptable thermal distortion because of its low coefficient of expansion even though difficult to fabricate. Titanium has good fatigue

resistance, and, like aluminum does not activate much. Copper base alloys and stainless steels, and low-expansion alloys such as Invar, are reported by Stark [1] as low-cost candidate structural materials for laser reactor mirrors.

Except for a calculation of the expected activation of candidate materials: 304 stainless steel, 6061 aluminum, and pure copper, for the HEGLF [1] by pulses of 4.5×10^{17} neutrons, with the sample located at 0.305 m from a source of 14-Mev neutrons, no neutronics and photonics studies of the expected behavior of materials for laser mirrors has been reported in the literature. The best available basis for comparing candidate materials for laser mirrors under neutron irradiation effects is in terms of the neutron and gamma heating, displacements per atom (dpa), helium from α-producing transmutations, and hydrogen from (n,p) and other hydrogen isotope production reactions. Kulcinski, Doran, and Abdou [3] presented a set of calculations comparing the response of several alloys of potential interest in a single conceptual fusion reactor spectrum. Gabriel, Bishop and Wiffen [2] also presented a set of calculations of the neutronic response of a number of elements and alloys to a particular projected fusion reactor first wall neutron spectrum, where they used more recent neutron cross-section data. Since the neutron spectrum seen by the mirror will be very different from that seen by the first wall, (because of the different compositions and configurations), and since heating estimates were not reported, as well as the gas production rates for some elements, the present study was undertaken. At the back of the mirror, materials responses were found to agree only in relative magnitudes with previous related results [2] for first wall materials and blanket spectra. However, they differ

at the mirror face due to a predominance there of the high energy neutron components over the slow ones, which in turn predominate at the mirror's back-side. The geometry also affects the results: here a point conical source in spherical geometry is used, whereas a cylindrical volume source in cylindrical geometry was used in previous related work [2] .

2. CALCULATIONAL MODEL

The materials chosen for analysis include elements that are of potential use as structural materials for laser power reactor mirrors, namely, Al, Fe, Cu, Mo and Ti. For a conceptual laser power reactor design, a typical off-axis parabolic mirror emplaced at 15 m from the center of the reactor cavity was considered [6]. Its thickness was taken as 35 cm. The first 2.5 cm are a solid plate of the considered structure, and the rest of the structure was considered as a honeycomb structure of the same material, cooled with water. A 5 v/o metal and 95 v/o H_2O ratio was considered there. Such a mixture will act as a shielding element to the 14-Mev neutrons hitting the mirror and the inelastic scattering gammas generated by them. If a lesser amount of water is used, it must be substituted by adequate shielding at the back of the mirror, say, concrete. That shielding will act in a manner similar to the water-metal mixture in slowing down neutrons and backscattering them to the mirror face; so that the present results still apply. Almost the same amount of cooling will be required in the concrete case, and care must be taken to avoid concrete decomposition by loss of evaporable water (20-200°C), of chemically constituted water (200-600°C),of carbon dioxide (650°C), melting (1100 ± 20°C), or liquifaction (1400 ± 50°C). Coating materials being of the order of a millimeter thickness [15], and consequently almost transparent to the 14-Mev neutrons, were not included in the calculations.

All calculations have been performed for an impinging 14-Mev neutron source. A two-dimensional Monte Carlo calculation considering a conical section of a one steradian solid angle (cone half angle $\theta_c = 32.7705°$) surrounded by a black absorber with spherical shells representing the mirror regions was considered. The 14-Mev neutron source was sampled isotropically at the head of the cone. A one-dimensional spherical geometry calculation would not have adequately modelled the system since it would have generated a significant backscattered radiation component. The mirror will mostly see a line-of-sight 14-Mev neutron flux, with the backscattered component mostly absorbed by the lining of the laser beam ports. Spherical or cylindrical one-dimensional calculations using conceptual designs first wall and blanket spectra [2,3] would then have not modelled the system adequately. The neutron source in this work is the average number of neutrons released in the fusion microexplosion per second. The total energy released per second is assumed to be 3000 MJ for a laser energy of 150 MJ at a repetition rate of 20 Hz. This corresponds to a source term of:

$$S = 3 \times 10^{9} \left(\frac{\text{Joules}}{\text{sec}}\right) \times \frac{1}{1.6021 \times 10^{-13}} \left(\frac{\text{Mev}}{\text{Joules}}\right) \times \frac{1}{17.62} \left(\frac{\text{source neutrons}}{\text{Mev}}\right) =$$

$$1.062737 \times 10^{21} \left(\frac{\text{source neutrons}}{\text{sec}}\right)$$

for a 4π solid angle.
Since the mirror sees a 14-Mev impinging flux, quantities of interest at the face of the mirror will scale as $1/R^2$ for mirrors emplaced at other distances R from the center of the cavity.

The combinatorial geometry capability of the MORSE Monte Carlo code [10,11] was used in modeling the problem geometry. The face plate of the mirror was divided into two regions of 0.5 and 2 cm thickness respectively, while the honeycomb water-metal mixture was divided into three regions of 7.5, 10, and 10 cm thickness respectively. Volume detectors were used to estimate the integrated quantities of interest [8, 9, 10].

A coupled 25-21 multigroup neutron-gamma cross-section set was used in the calculations. The group structure has been reported in reference [8]. This is a collapsed set from the EPR 100-group neutron and 21-group gamma-ray cross section library [12, 14], in turn considering data from the ENDF/B-IV file. The methods used to calculate the irradiation response of elements of interest have been described in detail in Reference 4. Reaction cross sections of interest were adopted from References 5 and 13.

The distribution in the polar angle θ for the conical point isotropic source of half angle θ_c was taken as:

$$P(\theta) = \frac{\int_0^{2\pi}\int_0^{\theta} \sin\theta' d\theta' d\psi}{\int_0^{2\pi}\int_0^{\theta_c} \sin\theta' d\theta' d\psi} = \frac{1 - \cos\theta}{1 - \cos\theta_c}$$

which requires sampling θ as:

$$\theta = \cos^{-1}\left[1 - \rho_1 (1 - \cos\theta_c)\right]$$

where ρ is a uniformly distributed random number over the interval [0, 1]. The azimuthal angle ψ was sampled between $\pm \Pi$ as:

$$\psi = \Pi (2\rho_2 - 1)$$

which implies the following formulae for the direction cosines u, v, w:

$$w = \cos\theta = 1 - \rho_1 (1 - \cos\theta_c)$$

$$s = \sin\theta = \sqrt{1 - \cos^2\theta} = \sqrt{1 - w^2}$$

$$\psi = \Pi (2\rho_2 - 1)$$

$$v = \sin\theta \sin\psi = s. \sin\psi$$

$$u = \sin\theta \cos\psi = s. \cos\psi$$

Table 1 shows the identification of the elements used in the calculation, their densities and atomic or molecular weights and the corresponding nuclear densities.

Coupled neutron-gamma multigroup Monte Carlo calculations were carried out using for each considered material 10 experiments of 50 particles each, totalling 500 histories. For the type of survey studies we are carrying out, this was found to be adequate. A typical CPU running time was 25 min on the University of Wisconsin UNIVAC-1110, for the Titanium case. Much of the time expenditure was in tracking the gamma photons and the thermalized neutrons, particularly in the metal-water mixture. For the Titanium case for example, 5424 scatterings occurred in the metal medium, whereas 322379 scatterings occurred in the water-metal mixture, over 500 histories.

3. RESULTS OF CALCULATIONS AND DISCUSSION

The scalar neutron and gamma fluxes are shown in Figures 1 to 5 for the Al, Cu, Fe, Mo, and Ti structure respectively since this is helpful in understanding the irradiation behaviour. The 14-Mev-group and the thermal-group neutron fluxes are displayed separately. The 14-Mev-group fluxes as

Table 1

Identification and Nuclei Densities of Used Elements

Element	ENDF/B-IV MAT No.	ρ(gm/cc)	At. or Mol. Weight	Nuclei Density (10^{24}/cc)
Al-27	1193	2.699	26.98	0.0602
Cu	1295	8.94	63.54	0.0848
Fe	1192	7.86	55.85	0.0848
Mo	1287	10.20	95.95	0.0640
Ti	1286	4.50	47.90	0.0566
O-16	1276	1.00	18.016	0.0335
H†	1269			0.0670

†Water bound hydrogen cross sections were used.

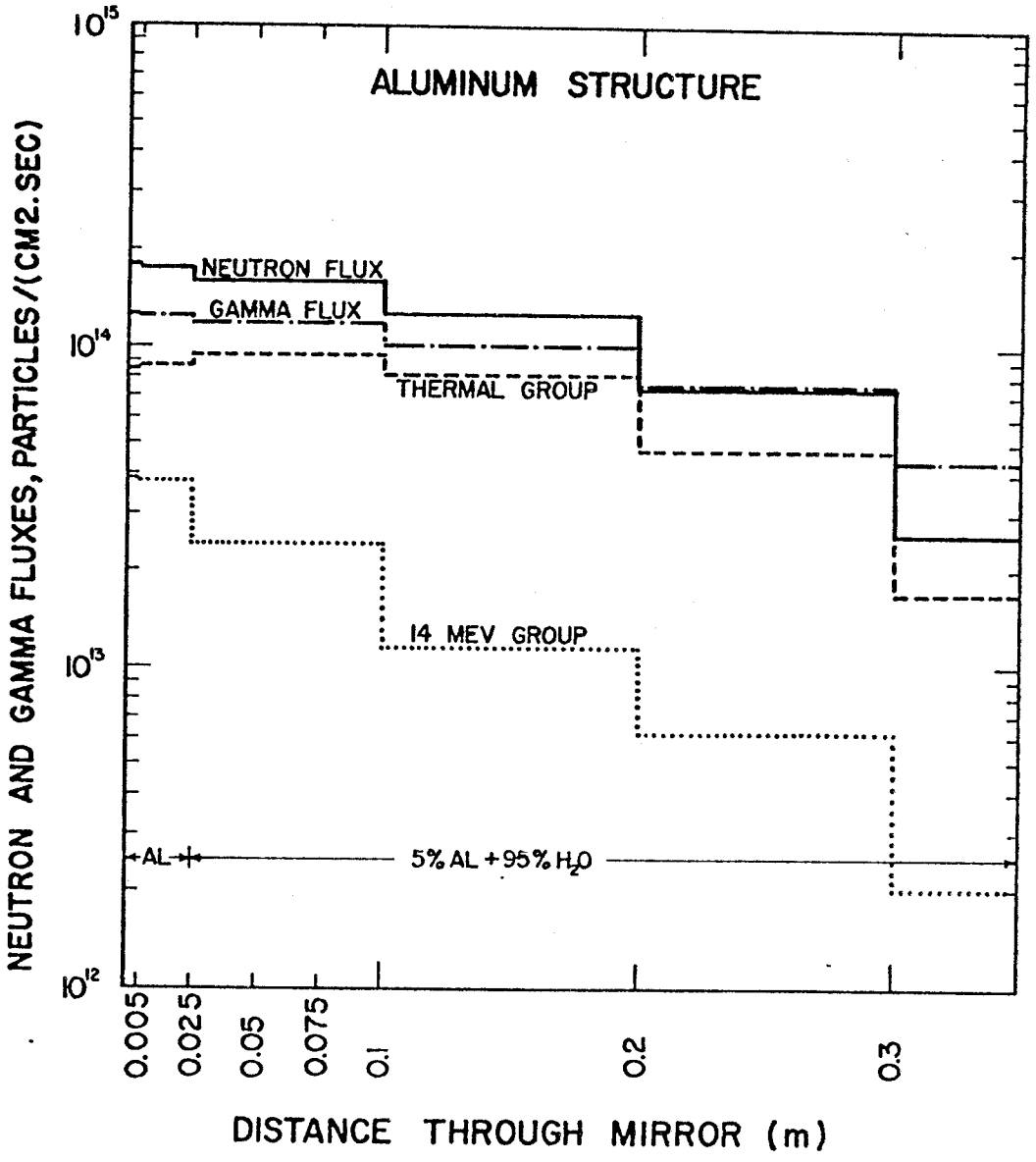
ALUMINUM STRUCTURE
NEUTRON FLUX
GAMMA FLUX
THERMAL GROUP
14 MEV GROUP
AL
5% AL + 95% H2O
NEUTRON AND GAMMA FLUXES, PARTICLES/(CM2.SEC)
DISTANCE THROUGH MIRROR (m)
10^15
10^14
10^13
10^12
0.005
0.025
0.05
0.075
0.1
0.2
0.3

Figure 1

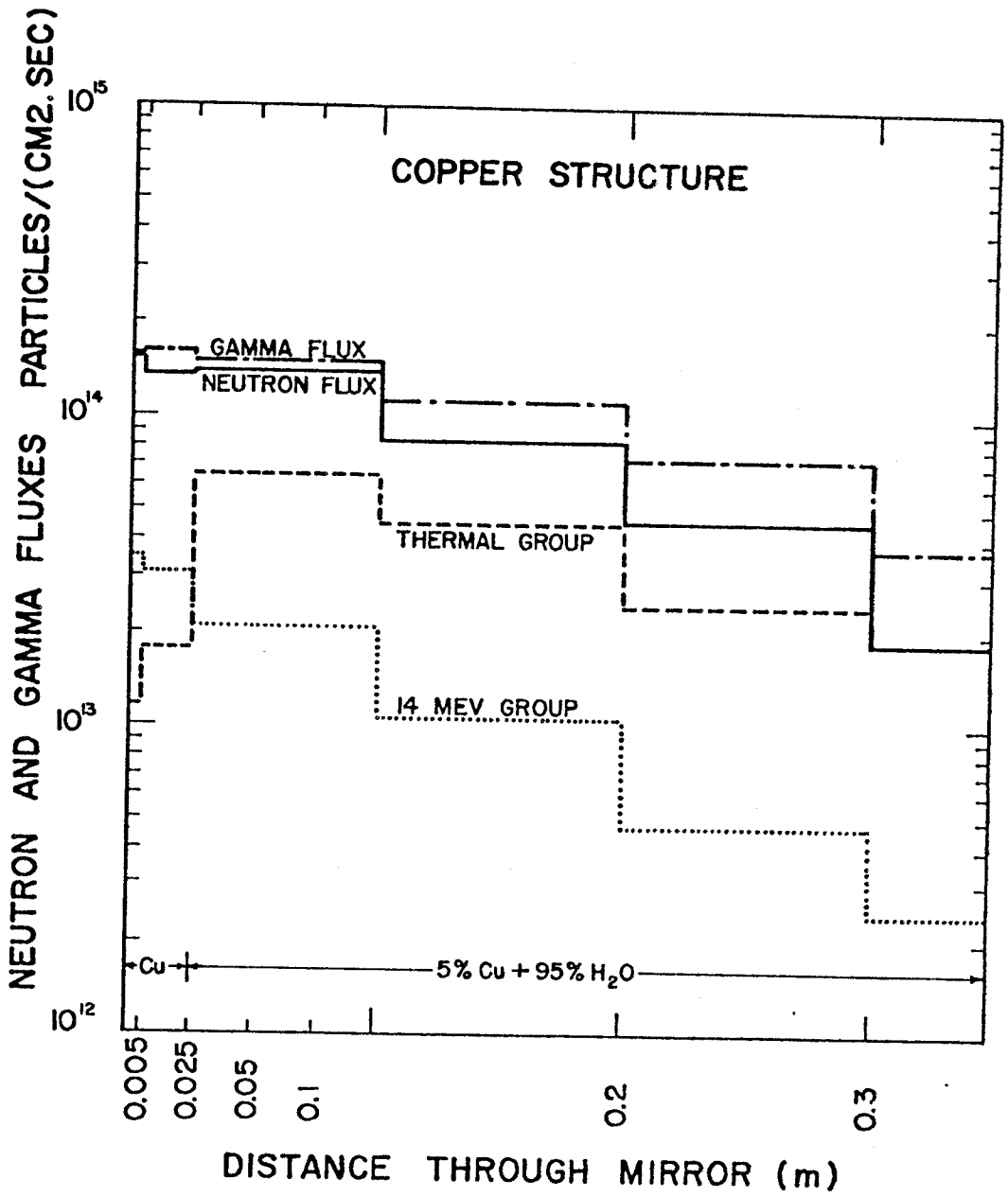
NEUTRON AND GAMMA FLUXES PARTICLES/(CM2. SEC)
10^15
10^14
10^13
10^12
COPPER STRUCTURE
GAMMA FLUX
NEUTRON FLUX
THERMAL GROUP
14 MEV GROUP
Cu
5% Cu + 95% H2O
0.005
0.025
0.05
0.1
0.2
0.3
DISTANCE THROUGH MIRROR (m)

Figure 2

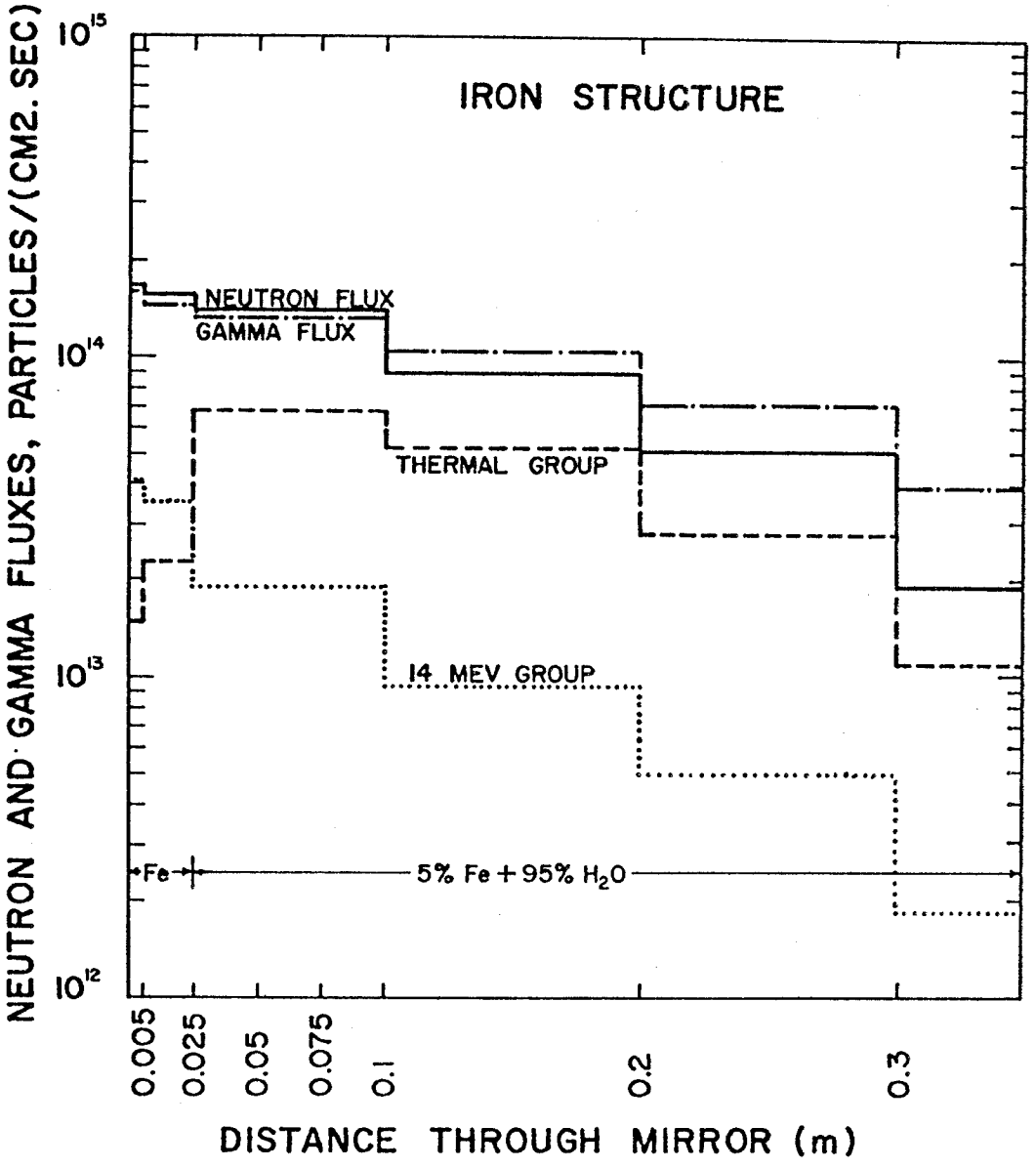
IRON STRUCTURE
NEUTRON FLUX
GAMMA FLUX
THERMAL GROUP
14 MEV GROUP
Fe
5% Fe + 95% H2O
NEUTRON AND GAMMA FLUXES, PARTICLES/(CM2. SEC)
10^15
10^14
10^13
10^12
0.005
0.025
0.05
0.075
0.1
0.2
0.3
DISTANCE THROUGH MIRROR (m)

Figure 3

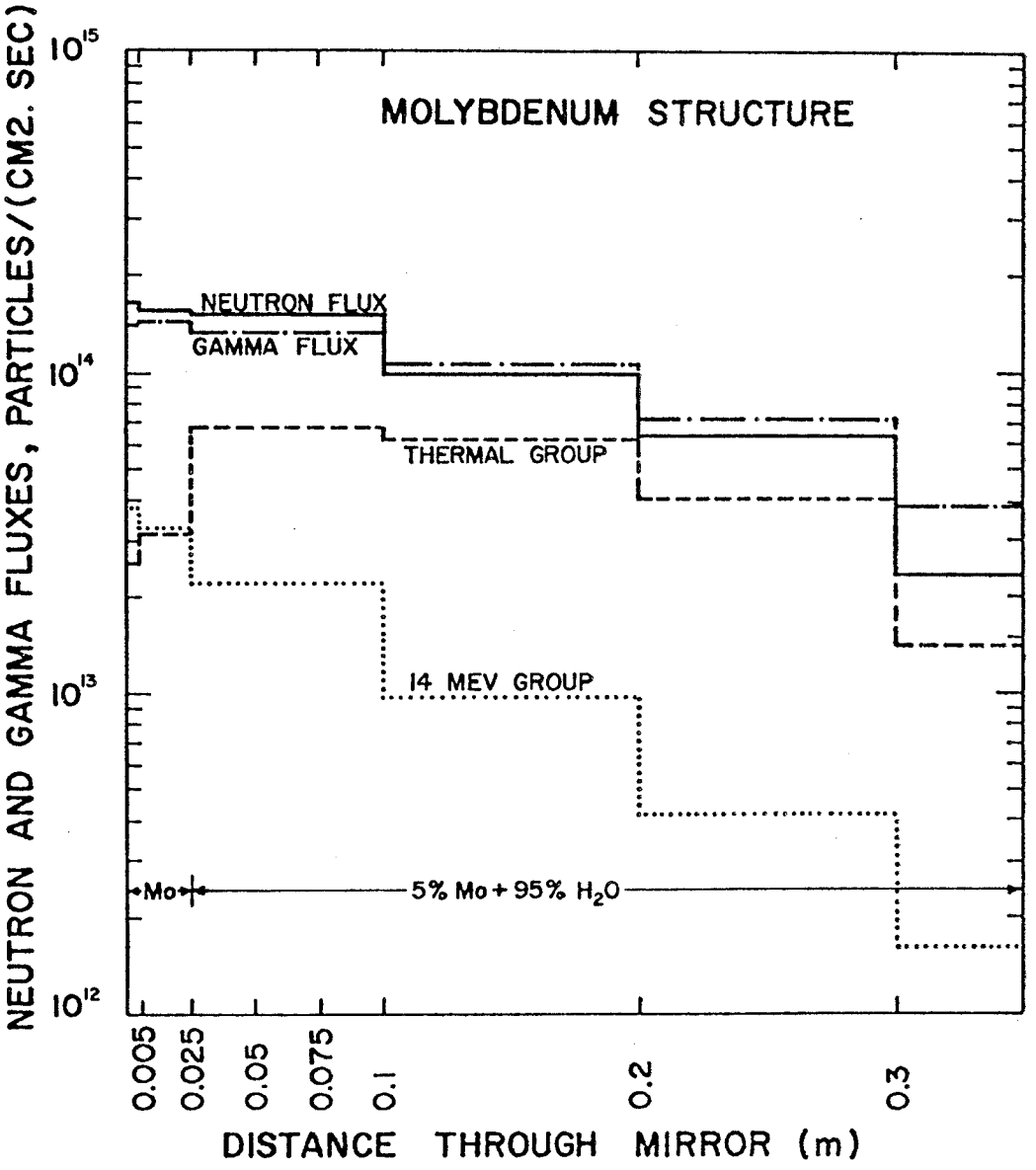
MOLYBDENUM STRUCTURE
NEUTRON FLUX
GAMMA FLUX
THERMAL GROUP
14 MEV GROUP
Mo
5% Mo + 95% H2O
NEUTRON AND GAMMA FLUXES, PARTICLES/(CM2. SEC)
10^15
10^14
10^13
10^12
0.005
0.025
0.05
0.075
0.1
0.2
0.3
DISTANCE THROUGH MIRROR (m)

Figure 4

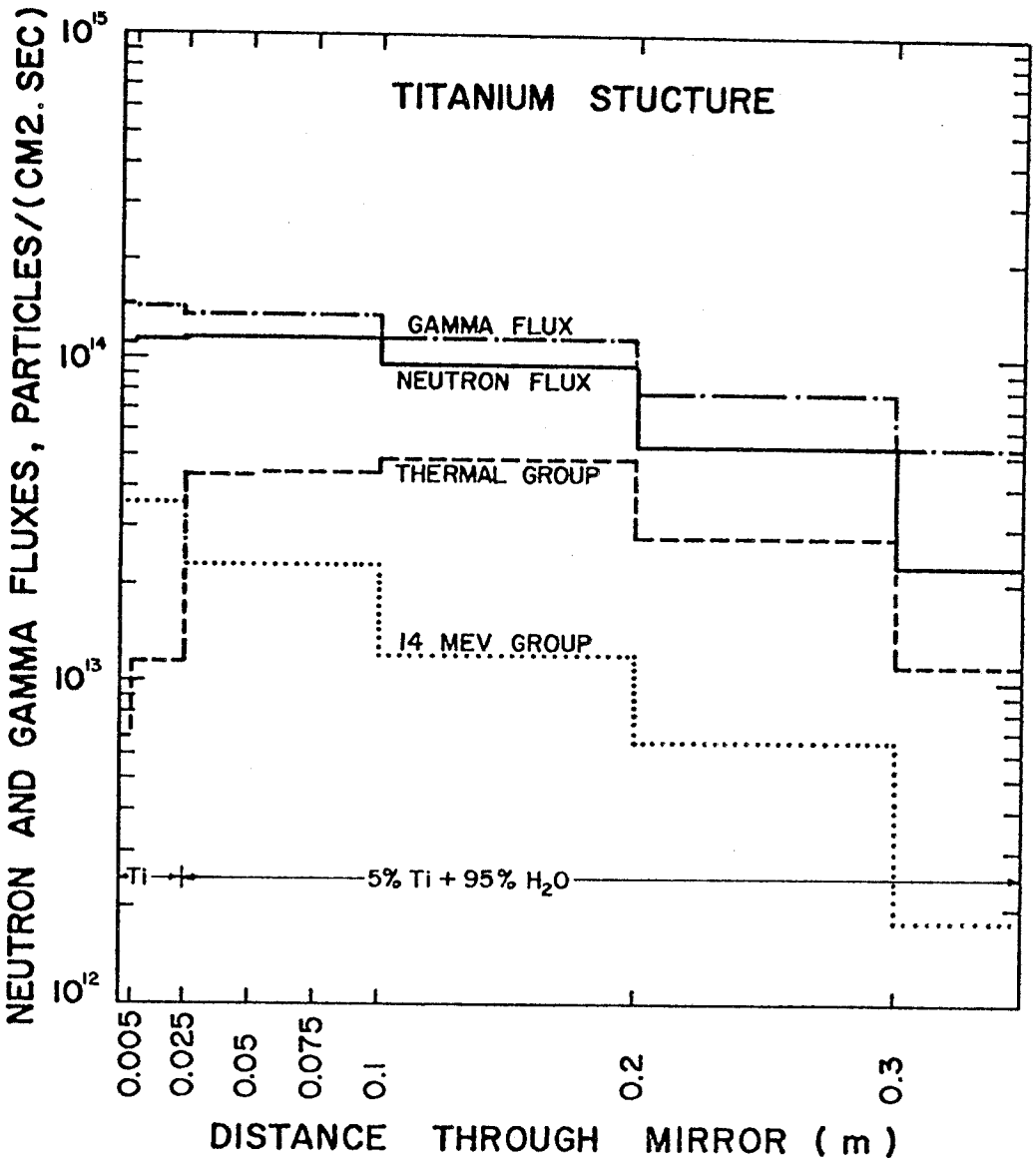
TITANIUM STUCTURE
GAMMA FLUX
NEUTRON FLUX
THERMAL GROUP
14 MEV GROUP
Ti
5% Ti + 95% H_2O
NEUTRON AND GAMMA FLUXES, PARTICLES/(CM2. SEC)
10^{15}
10^{14}
10^{13}
10^{12}
0.005
0.025
0.05
0.075
0.1
0.2
0.3
DISTANCE THROUGH MIRROR (m)

Figure 5

well as the gamma fluxes do not differ appreciably through the mirror for the materials considered. However, the thermal-group behaviour varies appreciably. The thermal-group flux peaks in the water-metal mixture behind the all-metal face, and dips in the latter. This behaviour resembles the behaviour in fuel elements in moderators in fission reactor work. In fact, the water acts here as a moderator and reflector to the source neutrons. The lowest dip in the thermal group flux occurs in Ti followed by Cu, Fe, Mo, and then Al. The highest peak thermal-group fluxes occur in reverse order from Al to Ti. The highest thermal-group leakage at the back of the mirror will be from Al, followed by Mo, Ti, Fe, then Cu. This also occurs for the total scalar neutron flux. Thus, an Al mirror will absorb neutrons the least, and a Cu one, the most. The least gamma leakage, however, will be from the Cu mirror followed by Mo, Fe, Al, then Ti. These remarks must be considered when designing the penetration shield.

In our calculations, the collision estimator was used in conjunction with region detectors to estimate the inner product (with summation over the energy groups):

$$x_v = \langle \Sigma_{rv}, \overline{\psi}_v \rangle \quad \left[\frac{\text{interactions}}{\text{source particle}}\right] \qquad (1)$$

where: $\Sigma_{rv} = N_v \sigma_r$ is a response function of interest $[cm^{-1}]$ in region v.

N_v is the nuclide number density of the considered element or mixture in [atoms/(barn·cm)] in region detector v.

σ_r is the microscopic cross section of the reaction of interest.

$\overline{\psi}_v$ is the volume integrated fluence in $\left[\frac{\text{interaction.cm}}{\text{source particle}}\right]$

v designates the region detector of interest.

For the estimation of the neutron and gamma fluxes, the response function Σ is input as a step function in the energy groups and regions of interest, and the volume averaged particle fluxes are estimated from:

$$\Phi_v = x_v \cdot \frac{S'}{\Sigma_{rv} \cdot V_v} \quad [\frac{\text{particles}}{\text{cm}^2 \cdot \text{sec}}] \tag{2}$$

where S'is the source term, and is equal to 1.06394×10^{21} [source particles/sec] multiplied by $\frac{d\Omega}{4\pi}$, where $d\Omega$ is the solid angle in which the source is sampled.

V_v is the volume of detector region v in [cm^3]

Σ_{rv} is the response function of interest in region v [cm^{-1}] (step function for estimation of fluxes).

For the estimation of heating rates, the σ_r's are replaced by the Kerma factors K_r, so that x_v is replaced by:

$$x'_v = \langle \Sigma'_{rv}, \bar{\psi}_v \rangle \quad [\frac{\text{ev}}{\text{source particle}}] \tag{3}$$

where $\Sigma'_{rs} = N_v \cdot K_r$ is the response function [$ev \cdot cm^{-1}$] in region v.

K_r is the Kerma factor in [barn•ev.].

To get the average volumetric heating rate in region v one uses:

$$q'''_v = x'_v \cdot \frac{S'}{V_v} \cdot C_q \quad [\frac{\text{Watts}}{\text{cm}^3}] \tag{4}$$

where S'is the source term in $[\frac{\text{source particles}}{\text{sec}}]$

V_v is the volume of region v in [cm^3].

$C_q = 1.6021 \times 10^{-13}$, is a conversion factor from ev to Joule.

The volumetric heating rates are necessary for the heat transfer cooling calculations. These are displayed for the various mirror structural materials in Figures 6 to 10. One notices that the neutron heating rate follows the shape of the thermal-group-neutron flux as displayed in Figures 1 to 5:

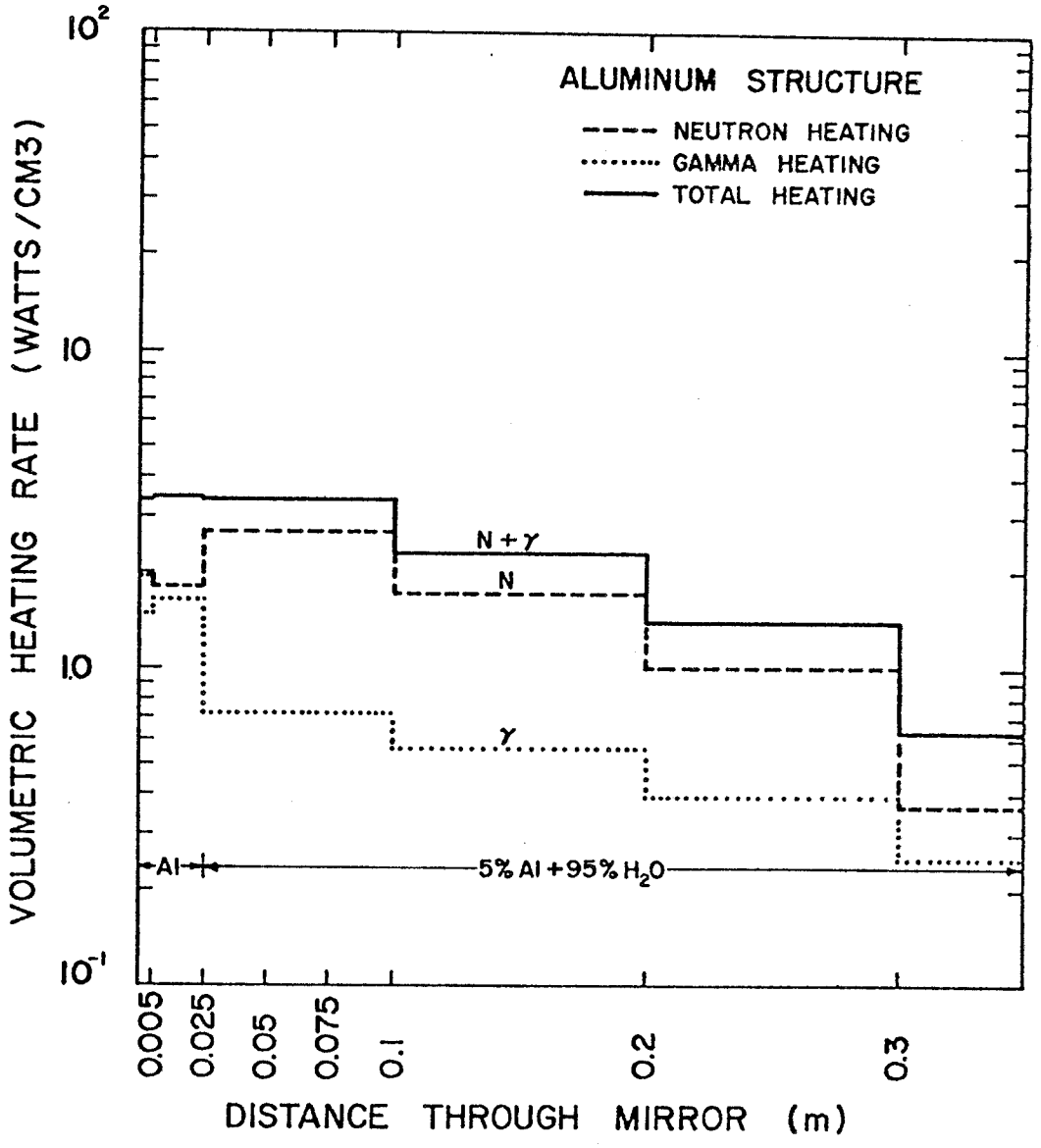
ALUMINUM STRUCTURE
NEUTRON HEATING
GAMMA HEATING
TOTAL HEATING
VOLUMETRIC HEATING RATE (WATTS/CM3)
10²
10
1.0
10⁻¹
N+γ
N
γ
Al
5% Al + 95% H₂O
0.005
0.025
0.05
0.075
0.1
0.2
0.3
DISTANCE THROUGH MIRROR (m)

Figure 6

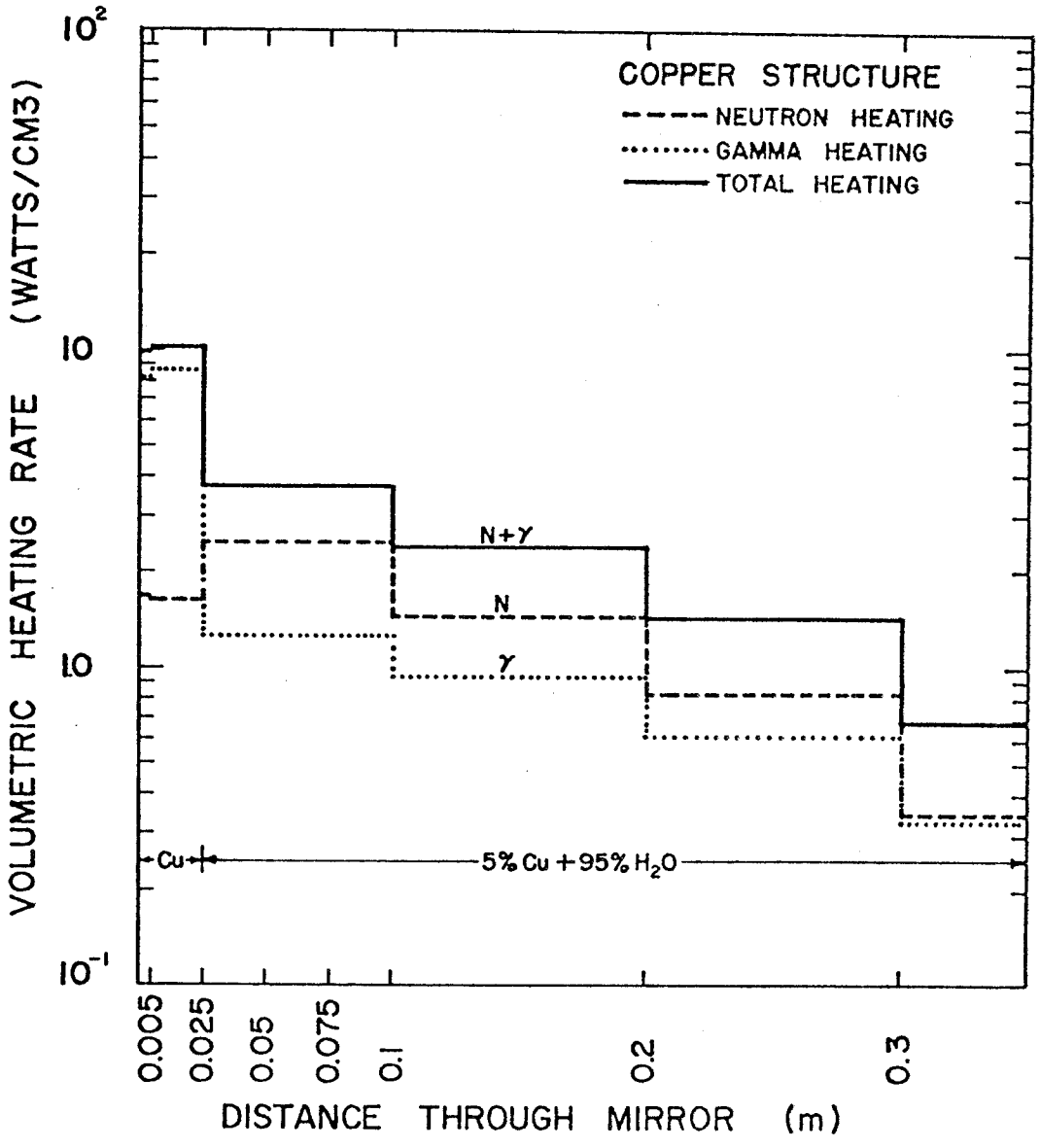
COPPER STRUCTURE
NEUTRON HEATING
GAMMA HEATING
TOTAL HEATING
VOLUMETRIC HEATING RATE (WATTS/CM3)
10²
10
1
10⁻¹
N+γ
N
γ
Cu
5% Cu + 95% H₂O
0.005
0.025
0.05
0.075
0.1
0.2
0.3
DISTANCE THROUGH MIRROR (m)

Figure 7

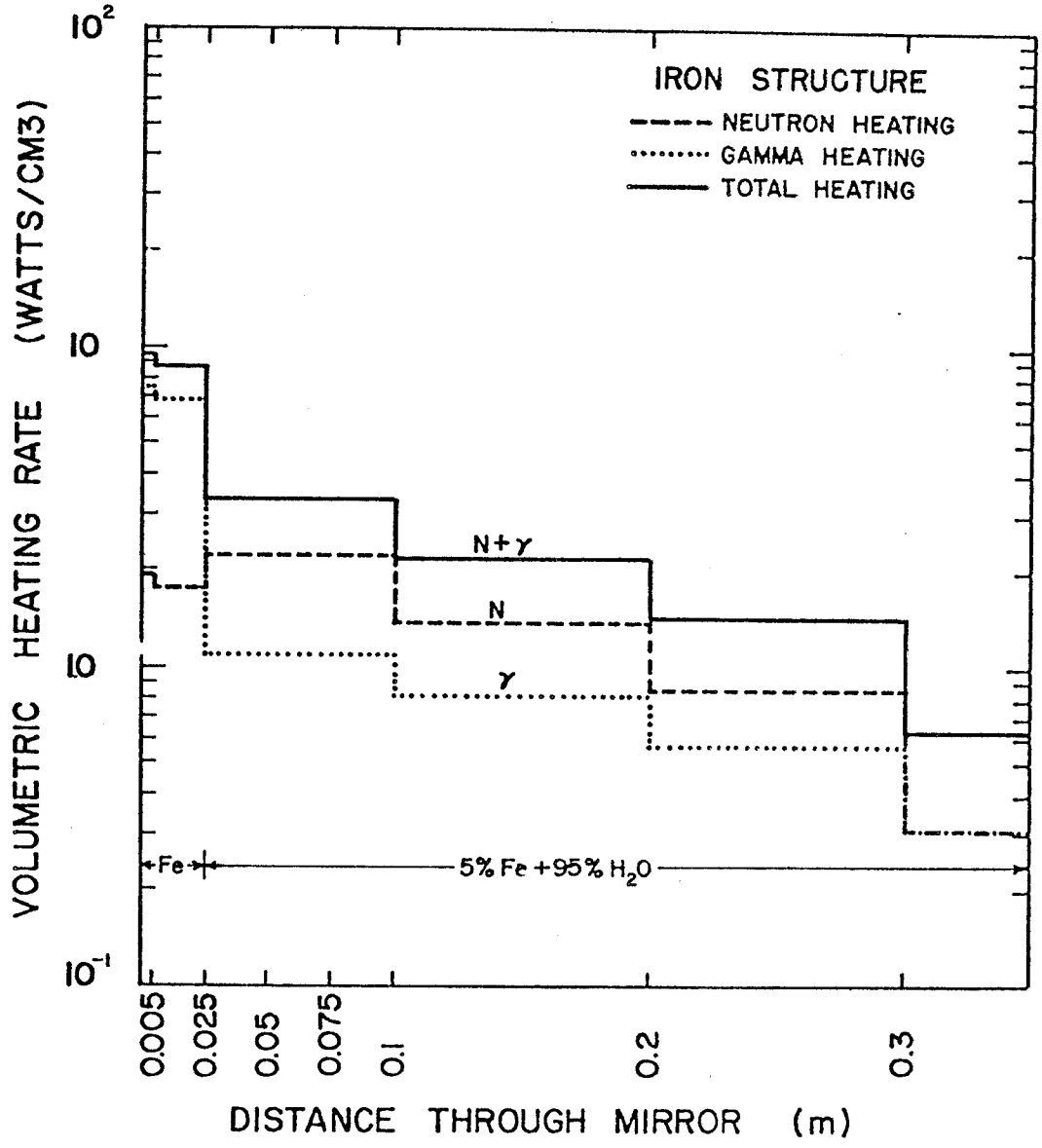
IRON STRUCTURE
NEUTRON HEATING
GAMMA HEATING
TOTAL HEATING
VOLUMETRIC HEATING RATE (WATTS/CM3)
10²
10
10
10⁻¹
N+γ
N
γ
Fe
5% Fe +95% H₂O
0.005
0.025
0.05
0.075
0.1
0.2
0.3
DISTANCE THROUGH MIRROR (m)

Figure 8

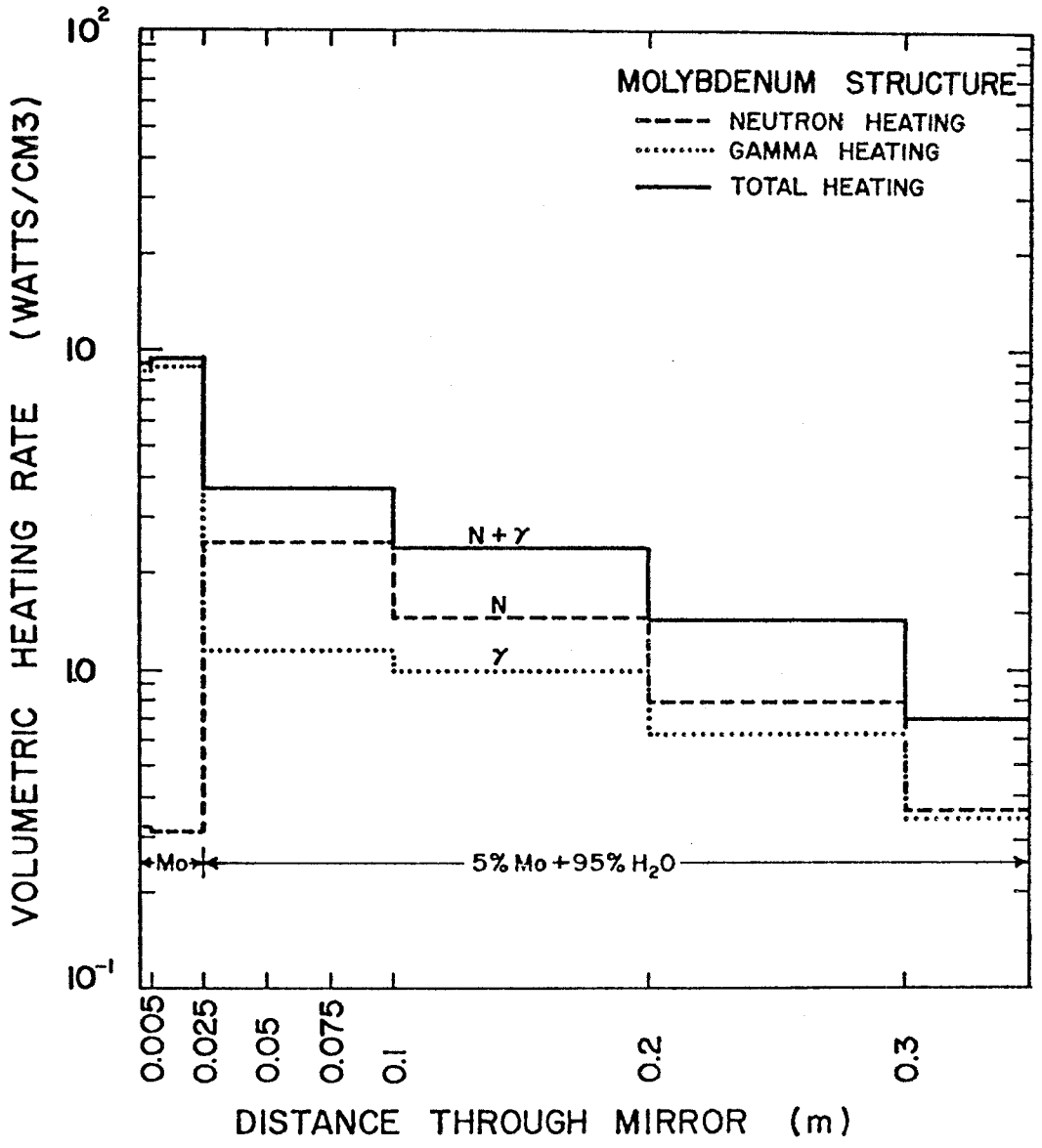
MOLYBDENUM STRUCTURE
NEUTRON HEATING
GAMMA HEATING
TOTAL HEATING
VOLUMETRIC HEATING RATE (WATTS/CM3)
10²
10
1
10⁻¹
N+γ
N
γ
Mo
5% Mo + 95% H₂O
0.005
0.025
0.05
0.075
0.1
0.2
0.3
DISTANCE THROUGH MIRROR (m)

Figure 9

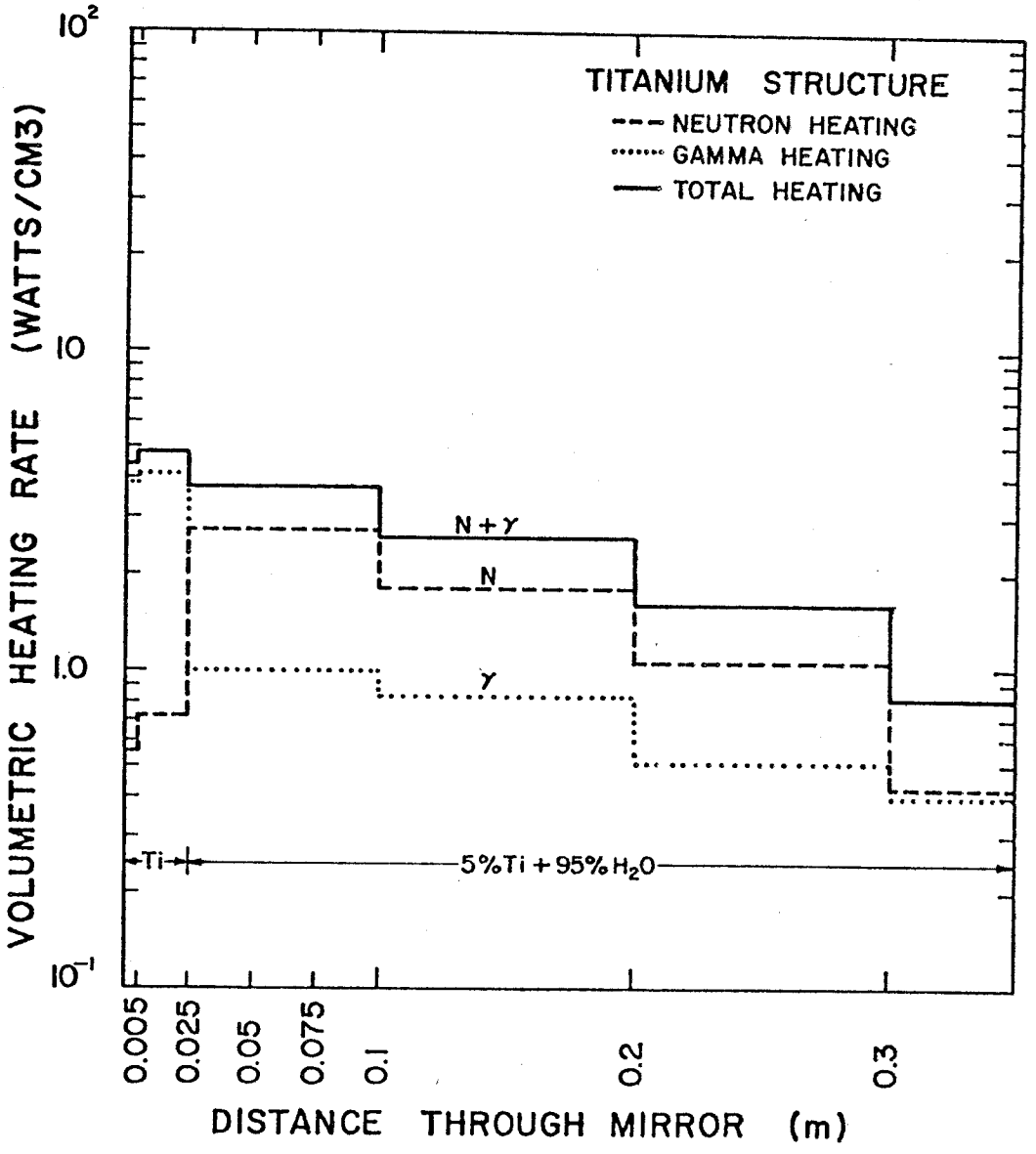
TITANIUM STRUCTURE
NEUTRON HEATING
GAMMA HEATING
TOTAL HEATING
VOLUMETRIC HEATING RATE (WATTS/CM3)
10²
10
1.0
10⁻¹
N+γ
N
γ
Ti
5%Ti + 95%H₂O
0.005
0.025
0.05
0.075
0.1
0.2
0.3
DISTANCE THROUGH MIRROR (m)

Figure 10

It peaks in the metal-water mixture, and dips in the all-metal mirror face. The neutron heating is larger than the gamma heating in the cooling structure. But the reverse occurs in the mirror face all-metal part, where the gamma heating largely exceeds the neutron heating, except for Al where they are almost of equal magnitude.

The total heating rate in the mirror face is largest in Cu followed by Mo, Fe, Ti, then Al, whereas it is almost of the same magnitude in the honeycomb water-cooled structure. This means that the temperature gradient will be lower in the case of Al and Ti than in the cases of Cu, Fe, or Mo. The thermal gradient will lead to dimensional distortion of the mirror if not corrected by appropriate orificing and controlled cooling of the mirror. Added to the neutron and gamma heating, provision must be made for the absorbed laser light, and further heating by the pellet X-rays and debris. Whereas neutrons and gammas affect the bulk structure, the others affect only the first few microns at the mirror face. For the laser pulse, Saito et al. [16] calculate the thickness Δx of the region of temperature rise as: $\Delta x = \sqrt{\frac{\pi}{4} \frac{Kt}{\rho c}}$; K is the thermal conductivity, ρ the density, c the specific heat, and t the width of the incident laser pulse. For a copper surface and a one-nanosecond pulse, $\Delta x = 0.35$ μm.

Figures 11 and 12 compare the estimated helium gas production rates from all helium producing reactions and hydrogen isotope production rates, respectively. Tables 2 and 3 display these values for the two regions of the mirror face: Region I comprising the first 0.5 cm of the mirror, while Region II comprising the next 2 cm. One estimated standard deviation of the mean is shown for these results.

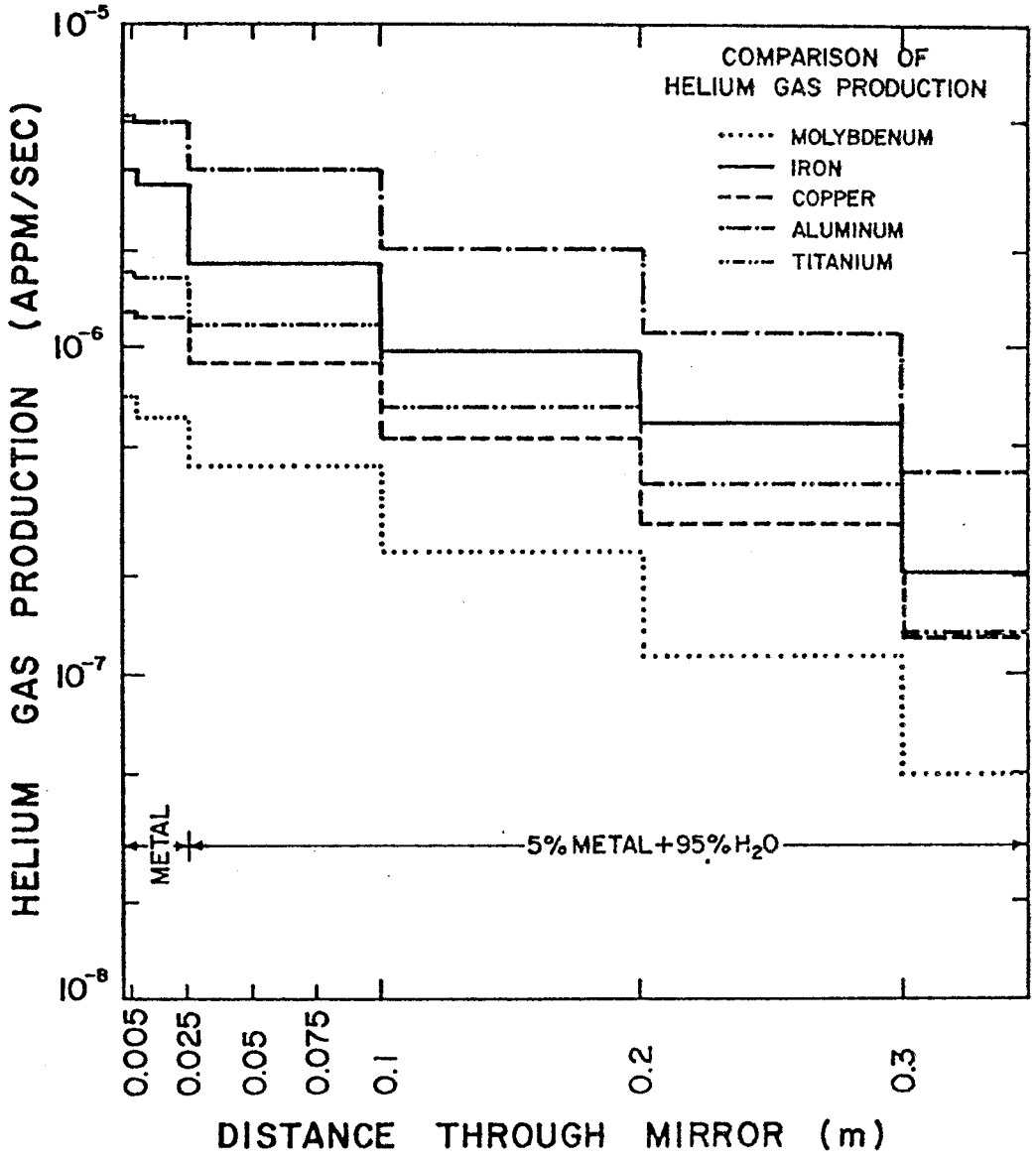
COMPARISON OF
HELIUM GAS PRODUCTION
MOLYBDENUM
IRON
COPPER
ALUMINUM
TITANIUM
HELIUM GAS PRODUCTION (APPM/SEC)
10^{-5}
10^{-6}
10^{-7}
10^{-8}
METAL
5% METAL+95% H_2O
0.005
0.025
0.05
0.075
0.1
0.2
0.3
DISTANCE THROUGH MIRROR (m)

Figure 11

Table 2

Helium Gas Production Rates (appm/sec) in Mirror Face

Structure	Region I	Region II
Al	(5.351396 ± 1.074025)-06	(5.016463 ± 0.435780)-06
Cu	(1.291910 ± 0.154655)-06	(1.241676 ± 0.082696)-06
Fe	(3.620044 ± 0.606357)-06	(3.239260 ± 0.205823)-06
Mo	(7.108789 ± 0.900257)-07	(6.158574 ± 0.430915)-07
Ti	(1.670791 ± 0.367273)-06	(1.576560 ± 0.122499)-06

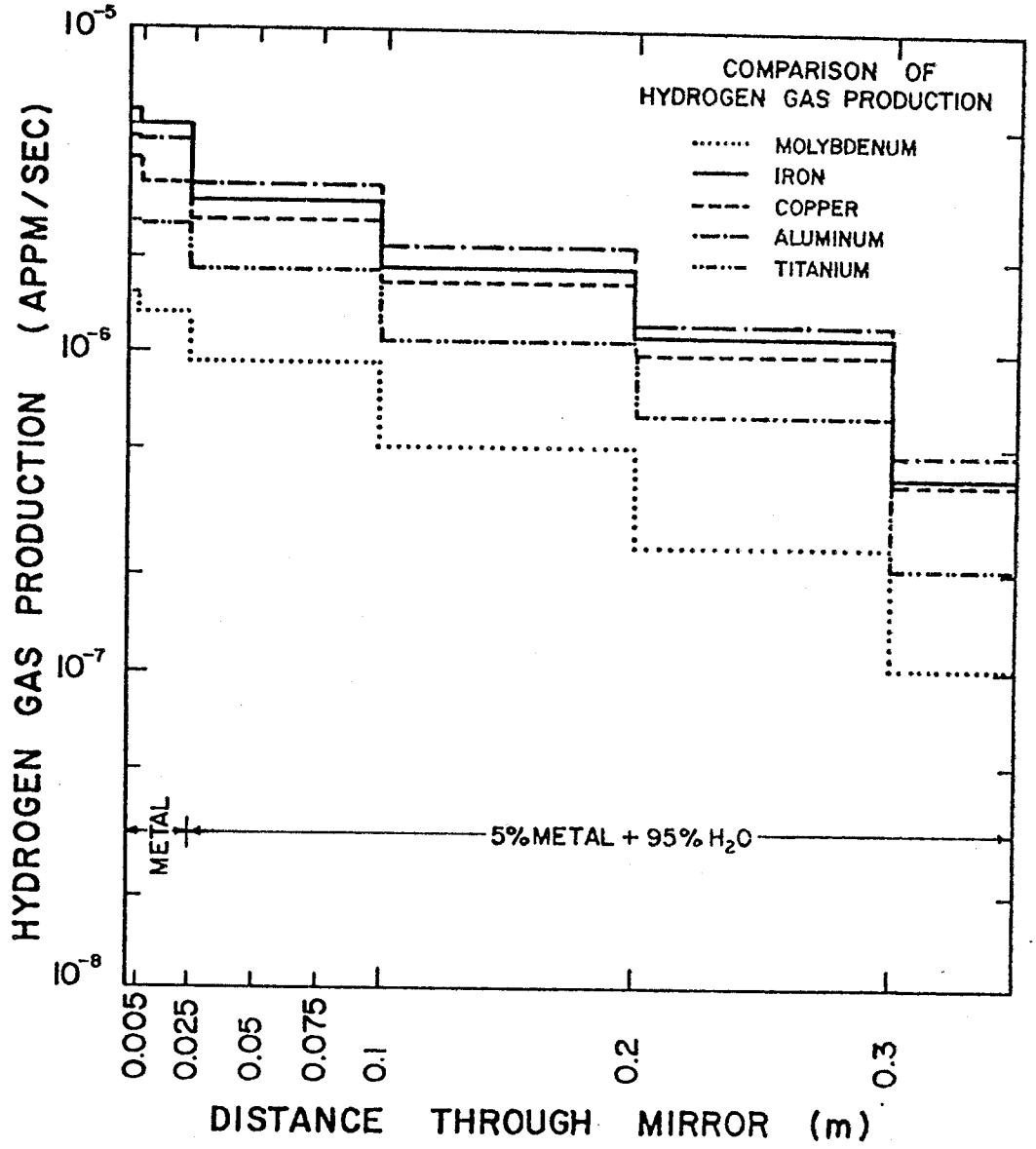
COMPARISON OF
HYDROGEN GAS PRODUCTION
MOLYBDENUM
IRON
COPPER
ALUMINUM
TITANIUM
HYDROGEN GAS PRODUCTION (APPM/SEC)
10^{-5}
10^{-6}
10^{-7}
10^{-8}
METAL
5%METAL + 95% H_2O
0.005
0.025
0.05
0.075
0.1
0.2
0.3
DISTANCE THROUGH MIRROR (m)

Figure 12

Table 3

Hydrogen Gas Production Rates (appm/sec) in Mirror Face

Structure	Region I	Region II
Al	(4.719977 ± 0.909904)-06	(4.572613 ± 0.393839)-06
Cu	(3.897110 ± 0.444972)-06	(3.341781 ± 0.207926)-06
Fe	(5.561190 ± 0.898132)-06	(5.060721 ± 0.376568)-06
Mo	(1.494898 ± 0.189344)-06	(1.293884 ± 0.090507)-06
Ti	(2.604744 ± 0.568824)-06	(2.469678 ± 0.192363)-06

For Σ_{rv} equal to the sum of gas production cross sections per unit volume, the gas production rates are estimated from:

$$G_v = x_v \cdot \frac{S'}{N_v \cdot V_v} \times 10^{-18} \quad [\frac{appm}{sec}] \qquad (5)$$

where the variables are as defined previously.

The He gas production rates vary from Al to Fe, Ti, Cu, then Mo over an order of magnitude. The hydrogen isotope gas production is of the same order of magnitude as the Helium gas production, but follows in magnitude a different order from highest to lowest (at the mirror face): Fe, Al, Cu, Ti, Mo.

Figure 13 compares the atomic displacements in (dpa/sec). Table 4 shows them with their associated standard deviations in Regions I and II of the mirror face. Cu will suffer the most (dpa/sec) at the mirror's face together with Ti, followed by Fe, then by Al and Mo.

For Σ_{rv} as the macroscopic atomic displacement cross sections, the atomic displacements rates are estimated from:

$$A_v = x_v \cdot \frac{S'}{N_v \cdot V_v} \quad [\frac{displacement}{atom.sec}] \qquad (6)$$

In the work of Gabriel, Auburgey and Greene [2], for first wall materials in a fusion reactor blanket neutron spectrum, the displacement damage magnitudes occur in the following order for the materials we have considered:

Ti, Cu, Al, Fe, Mo

From Figure 13, it can be noticed that at the back of the mirror, where the flux is predominantly soft, the same ordering in the magnitudes occurs. However, at the front of the mirror, a different ordering occurs:

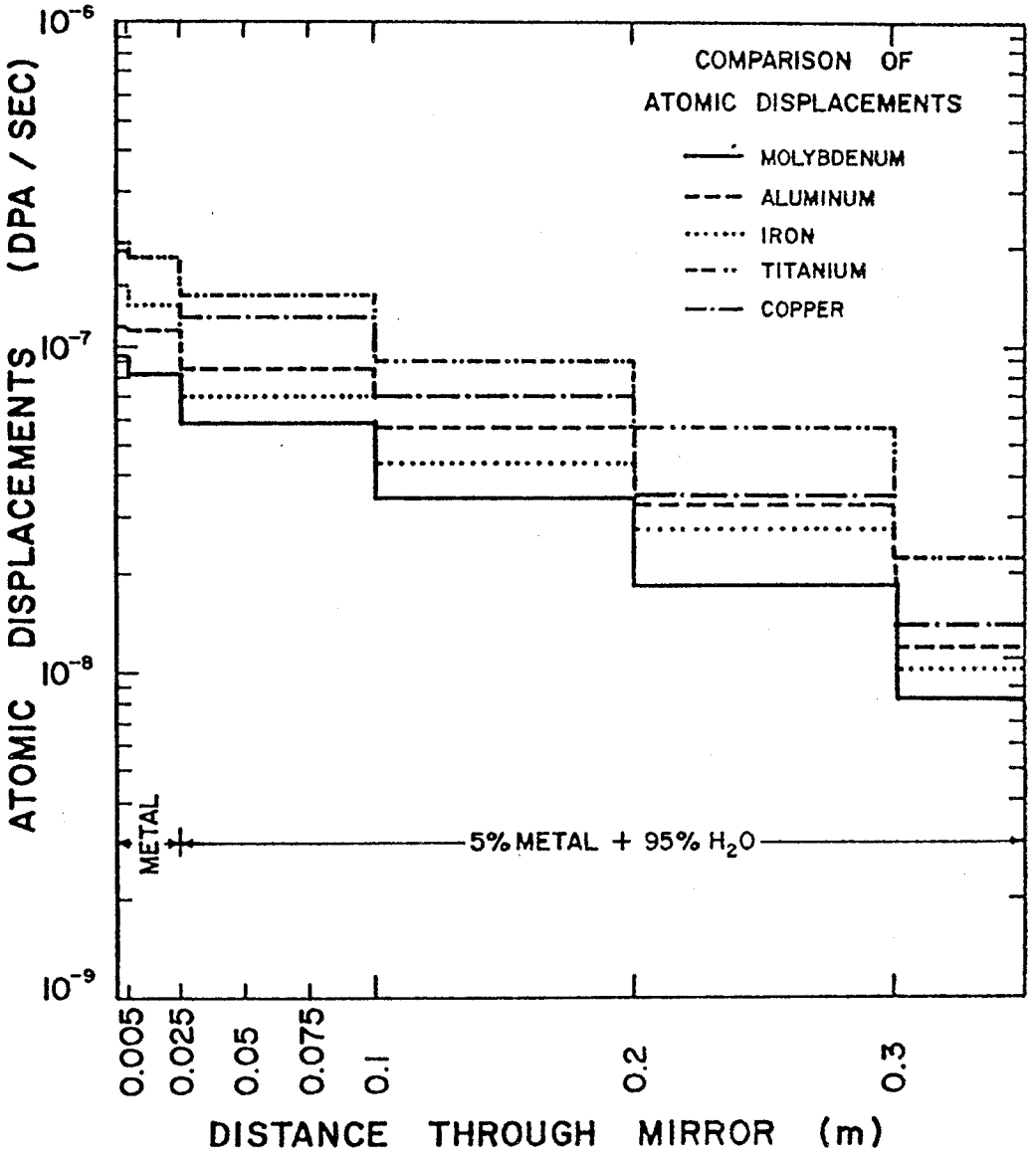
COMPARISON OF
ATOMIC DISPLACEMENTS
MOLYBDENUM
ALUMINUM
IRON
TITANIUM
COPPER
ATOMIC DISPLACEMENTS (DPA / SEC)
10^{-6}
10^{-7}
10^{-8}
10^{-9}
METAL
5% METAL + 95% H_2O
0.005
0.025
0.05
0.075
0.1
0.2
0.3
DISTANCE THROUGH MIRROR (m)

Figure 13

Table 4

Atomic Displacements Rates (dpa/sec) in Mirror Face

Structure	Region I	Region II
Al	(1.171044 ± 0.167459)-07	(1.135044 ± 0.090804)-07
Cu	(2.112372 ± 0.316856)-07	(1.819247 ± 0.127347)-07
Fe	(1.530206 ± 0.247893)-07	(1.347009 ± 0.109108)-07
Mo	(9.529783 ± 1.520078)-08	(8.323508 ± 0.634543)-08
Ti	(1.987894 ± 0.296634)-07	(1.981773 ± 0.134404)-07

Cu, Ti, Fe, Al, Mo

For the helium gas production in appm/sec in the work of Gabriel et al. [2] the magnitudes occur in the following ordering (no results were given for Mo):

Al, Fe, Ti, Cu

This also agrees with our results both at the front and back of the mirror, with Mo following Cu in the ordering, as shown in Figure 11.

For the hydrogen gas production Gabriel et al. [2] obtained magnitudes in the following ordering:

Cu, Fe, Al, Ti

while we obtained results at the back of the mirror from Figure 12 in the following order:

Al, Fe, Cu, Ti, Mo

and at the front of the mirror:

Fe, Al, Cu, Ti, Mo

The difference between the results at the front face of the mirror is to be expected since in our modeling, a predominantly 14-Mev-group neutron component affects it. The results of Gabriel et al. [2] consider a single particular first-wall neutron spectrum of a Tokamak designed to provide adequate tritium breeding without excessive tritium inventory. The different spectra for each mirror material were considered in our calculation, and this leads to different results. The results mostly agree in relative magnitudes at the back of the mirror where energy-degraded flux components predominate. Table 5 shows a comparison of results. Our results, even though of the same order of magnitude; give lower estimates since they consider a pure 14-Mev neutron component impinging normally on the first wall,

Table 5

Comparison of Mirror Face Neutronic Damage Response, to First Wall Response

Element	Displacement Damage (dpa/sec) x 10^{-7}		Helium Gas Production (appm/sec) x 10^{-7}		Hydrogen Gas Production (appm/sec) x 10^{-7}	
	First Wall†	Mirror Face*	First Wall	Mirror Face	First Wall	Mirror Face
Fe	3.62	1.17	34.90	36.20	151.00	55.60
Mo	2.38	0.95	-----	7.10	------	14.90
Ti	5.03	1.98	33.50	16.70	49.70	26.00
Al	4.63	1.17	101.00	53.50	94.50	47.20
Cu	4.88	2.11	31.80	12.90	173.00	38.90

† 1 MW/m^2 neutron energy loading on first wall, with blanket spectrum [2].

* 0.85 MW/m^2 neutron energy loading on mirror face, pure 14-Mev flux impinging on mirror.

on the assumption that the penetration shielding can be designed to intercept streaming and backscattered components from the blanket and shield. Also, our results correspond to a 0.85 MW/m^2 neutron wall loading, and are compared to those for a 1 MW/m^2 wall loading. Moreover, the adopted point source model in spherical geometry leads to shorter effective mean free paths at the face of the mirror than the previous related work [2], where a volume plasma source model in cyclindrical geometry is used.

Future investigations should consider specific mirror designs and take into account factors such as its alloy composition, spatial orientation, and the penetration shielding environment including the beam lining, and the shielding at the mirror back. The penetration design must be chosen to minimize the scattered components from the cavity and blanket reaching the mirror position.

4. SUMMARY

This work compares estimates of the neutron and gamma irradiation response of water cooled mirrors for contemplated Laser Fusion Power Reactors, for some candidate structural materials. The neutron and gamma response will affect the bulk of the structure, whereas the pellet X-rays and debris response will mostly affect the first 10 microns of the mirror face. Mo appears to suffer the fewest atomic displacements and gas production rates, but results in a high volumetric neutron and gamma heating. If easy to fabricate, it may be a good choice as a structural material due to its low coefficient of expansion. Al and Ti offer the least heating rates, but Al suffers the highest He gas production. Al and Ti offer the advantage of low activation, with some Ti alloys having good fatigue strength (e.g., Ti 6% Al, 6% V, 2% Sn). Ti, however, has a high atomic displacement damage potential. The highest hydrogen gas production will occur in Fe, and this effect may be amplified by the presence of Ni in any stainless steel alloy. Fe may also activate, substantially limiting

access to the mirror. Cu ,even though of high reflectivity to the laser light, and of good thermal conductivity, will have the highest atomic displacement rate and volumetric heating at the mirror face, added to its activation potential. Variations of the obtained estimates are within an order of magnitude for the quantities of interest. At the back-side of the mirror results mostly agree in relative magnitudes with previous results for first wall materials and blanket spectra, but differ substantially at the mirror face where the 14-Mev neutron component predominates.

REFERENCES

[1] Stark, E., "Laser Fusion Program", LA-6510-PR, Los Alamos Scientific Laboratory (1976).

[2] Gabriel, T. A., Bishop, B. L., and Wiffen, F. W., "Calculated Irradiation Response of Materials Using A Fusion-Reactor First-Wall Neutron Spectrum", ORNL-TM-5956, Oak Ridge National Laboratory (1977).

[3] Kulcinski, G. L., Doran, D. G., and Abdou, M. A., "Comparison of Displacement and Gas Production Rates In Current Fission and Future Fusion Reactors", p. 239 in "Properties of Reactor Structural Alloys After Neutron Or Particle Irradiation", ASTM STP 570, ASTM (1975).

[4] Gabriel, T. A., Auburgey, J. D., and Greene, N. M., "Radiation Damage Calculations: Primary Recoil Spectra, Displacement Rates, and Gas Production Rates", ORNL/TM-5160, Oak Ridge National Laboratory (1976).

[5] Avci, H., Kulcinski, G. L., "The Response of ISSEC Protected First Walls To DT and DD Plasma Neutrons", UWFDM-135, October (1975).

[6] Cooper, G., Howard, J., Personal communications, Fusion Research Program, The University of Wisconsin.

[7] Ragheb, M. H., Cheng, E. T., and Conn, R. W., "Monte Carlo Study Of Asymmetry Effects In A Lithium Oxide Blanket For A Laser Driven Reactor", UWFDM-207, University of Wisconsin (1977).

[8] Ragheb, M. M. H., Cheng, E. T., and Conn, R. W., "Comparative One-Dimensional Monte Carlo and Discrete Ordinates Neutronics And Photonics Analysis For A Laser Fusion Reactor Blanket With Li_2O Particles As Coolant and Breeder", UWFDM-193, University of Wisconsin (1977).

[9] Cheng, E. T., Ragheb, M. M. H., and Conn, R. W. "Neutronics and Photonics Studies For The University of Wisconsin Laser Fusion Reactor Blanket", Trans. Am. Nucl. Soc., 26, 504 (1977).

[10] Ragheb, M. M. H., and Maynard, C. W., "A Version Of The MORSE Multigroup Transport Code For Fusion Reactors Blankets And Shield Studies", BNL-20376, Brookhaven National Laboratory (1975).

[11] RSIC Code Package CCC-203, "MORSE-CG", Radiation Shielding Information Center, ORNL (1976).

[12] Ford III W. E., Santoro, R. T., Roussin, R. W. and Plaster, D. M., "Modification Number One To The Coupled 100n-21 Gamma Cross Section Library For EPR Calculations", ORNL/TM-5249 (1976).

[13] Abdou, M. A., and Roussin, R. W., "MACKLIB, 100 Group Neutron Fluence-to-Kerma Factors And Reactions Cross Sections Generated By The MACK Computer Program From Data In ENDF Format", ORNL-TM-3995 (1974).

[14] Plaster, D. M., Santoro, R. T., and Ford III, W. E., "Coupled 100-Group Neutron and 21-Group Gamma-Ray Cross Sections For EPR Calculations", ORNL-TM-4872 (1975).

[15] Reichelt, W. H., Blevins, D. J., and Turner, W. C., "Metal Optics In CO_2 Laser Fusion Systems", LA-UR-77-468 (1977).

[16] Saito, T., Milam, D., Baker, P., Murphy, G., NBS Special Publication #435, 29 (1975).